# Generating synthetic wind loading time-series: some application for wind-induced fatigue assessment.

*Pierre Verhaeghe, Technical Director, pierrev@holmesgroup.com*


## ABSTRACT

*Synthetic wind loading time series are generated and analyzed for wind fatigue using the rainflow algorithm. The fatigue damage distribution for very dynamic structures is shown to match the closed-form Rayleigh distribution usable for a narrow-band process, which forms the basis of the cycle counts shown in AS / NZS1170.2 but differs more significantly for less dynamic structures. Reduction factors applied to stress are suggested to compensate for this, which could be directly implemented in an existing method.*


## INTRODUCTION

Closed-form solutions to evaluate wind fatigue have become available in the literature with various levels of accuracy and complexity, but detailed fatigue assessment still potentially requires the use of the rainflow counting method applied on simulated loading time-histories. Essential reading on the subject is (Wyatt, 2004). The article below revisits aspects of this work and complements it with additional parametric studies. It highlights the potential conservatism in the cycle counts in AS / NZS1170.2 for moderately dynamic structures. It tentatively proposes reductions applicable to the method recently proposed by (Holmes et al., 2012) subject to additional checks.

## SYNTHETIC WIND LOADING TIME SERIES

Correlated wind gust speeds time-series are generated using an autoregressive model, which coefficients are calculated using the Yule-Walker equations and the Von-Karman auto-correlation function normally used to describe the correlation in wind gust mechanisms. Sets of twenty hours of wind speeds at 0.1s interval with 22% turbulence intensity and various mean wind speeds are generated. The gust speeds are found to follow a gaussian probabilistic distribution, with the required Von-Karman spectrum. The wind loads are generated by successively applying Fourier and Inverse Fourier Transform, and the Aerodynamic and Mechanical Admittance functions, assuming a linear mode-shape and uniform mass distribution. The dynamic factor $C_{dyn}$ evaluated from the time series is found to match that calculated using the Standard for Wind Loading AS / NZS 1170.2. The average wind speeds, tributary area, natural frequency and damping can be adjusted for the parametric studies.

## FATIGUE DAMAGE DISTRIBUTION PER STRESS LEVEL

Using the Miner quotient, the contribution of a stress range S to the total wind fatigue damage can be defined as:

$$Q_S = n / N \qquad (1)$$

where n is the demand, i.e. the number of cycles of stress range S during the lifetime of the structure. N is the capacity, i.e. the number of cycles of stress S alone resulting in failure. Typically, N is evaluated using the bi-slope S-N curves available in structural design documents.

On this basis, Equation (1) can then be rewritten as:

$$Q_S = A\ n\ S^m \qquad (2)$$

where A is a constant, which depends on the structural detail. m varies from 3 to 5 depending on the on position on the S-N curves. In this study, m is set equal to 3. As per Wyatt [1], there is a significant number of cycles at very low stress, which contribute little to the damage. The damage distribution is therefore better assessed by normalizing the stress range. Following (Wyatt, 2004) notation, we define:

$$n_{4\sigma} = n_S\ (\ S\ /\ 4\sigma\ )^m \qquad (3)$$

$\sigma$ is the rms of the stress time series. $n_{4\sigma}$ is the equivalent number of cycles at a stress range equal to $4\sigma$, which results in the same fatigue damage as $n_S$ cycles of stress range equal to S.

The synthetic wind loads are analyzed for various inputs parameters using the rainflow algorithm, separately for the total response, the broad-band and narrow-band components both taken in isolation. The histograms below provide the distribution in terms of $n_{4\sigma T}$ (Equ 3). The stress range is normalized using $\sigma_T$ , i.e. rms of the total response. The plot on the left is for a moderately dynamic structure ($\sigma_N / \sigma_B = 0.6$). The plot on the right is for significantly more dynamic ($\sigma_N / \sigma_B > 1.5$).

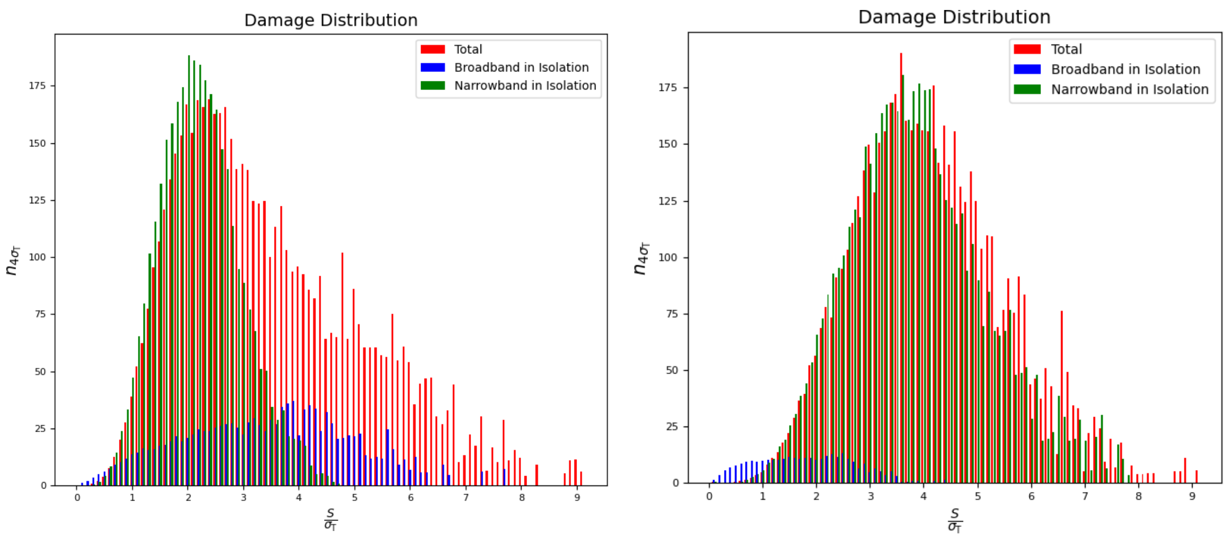


**Figure 1. Distribution of fatigue damage for a moderately (left) and very dynamic structure (right)**

The broad-band component alone (shown in blue) would cause considerably less fatigue damage than the narrow-band component (shown in green) if each were considered separately. The stress range contributing the most to the damage varies from about two to four times $\sigma_T$ for the more dynamic structure. For the moderately dynamic structure (left) and at a stress range around $2\sigma_T$, the number of cycles from the narrow-band component added to that of the broad-band component exceed the number cycles of the total response. However, the total response has significantly more cycles at higher stress levels. This indicates a redistribution of the cycles from the lower to higher stress ranges, as the narrow-band component is superimposed on that of the broad-band. This mechanism considerably increases the damage from that of the narrow-band in isolation.

## NORMALIZED FATIGUE RATE

(Wyatt, 2004) introduced a normalized fatigue rate as follows:

$$\tilde{n}_{4\sigma T} = n_{4\sigma T}\ L_1\ /\ \bar{U} \qquad (4)$$

with $L_1$ the integral length scale and $\bar{U}$ the mean speed. A parametric study of $\tilde{n}_{4\sigma T}$ was completed for a range of tributary area, natural frequencies and damping. The plot shown below is obtained by reducing the natural frequency while keeping the damping equal to 1%. The curves tend to reach a maximum for $\sigma_N$ / $\sigma_B$ equal to 0.6, i.e. for moderately dynamic structures. The fatigue damage accumulates relatively faster when the rms of the narrow-band component is slightly larger than half that of the broad-band component. As the structure becomes more dynamic, i.e. as $\sigma_N$ / $\sigma_B$ increases, the narrow-band component dominates the response, and the fatigue rate reduces as does the natural frequency. Note this curve differs from that shown in (Wyatt, 2004) which shows a monotonical increase of $\tilde{n}_{4\sigma T}$ with $\sigma_N$/ $\sigma_B$. A similar result to that of (Wyatt, 2004) is reached if the variation in $\sigma_N$/ $\sigma_B$ is obtained by reducing the damping and keeping the natural frequency fixed. Unless a damping device is used, designers would more likely select a fixed conservative value for damping, while the natural frequency would vary depending on the structural solution adopted. The presentation below might therefore be more readily useful for designers.

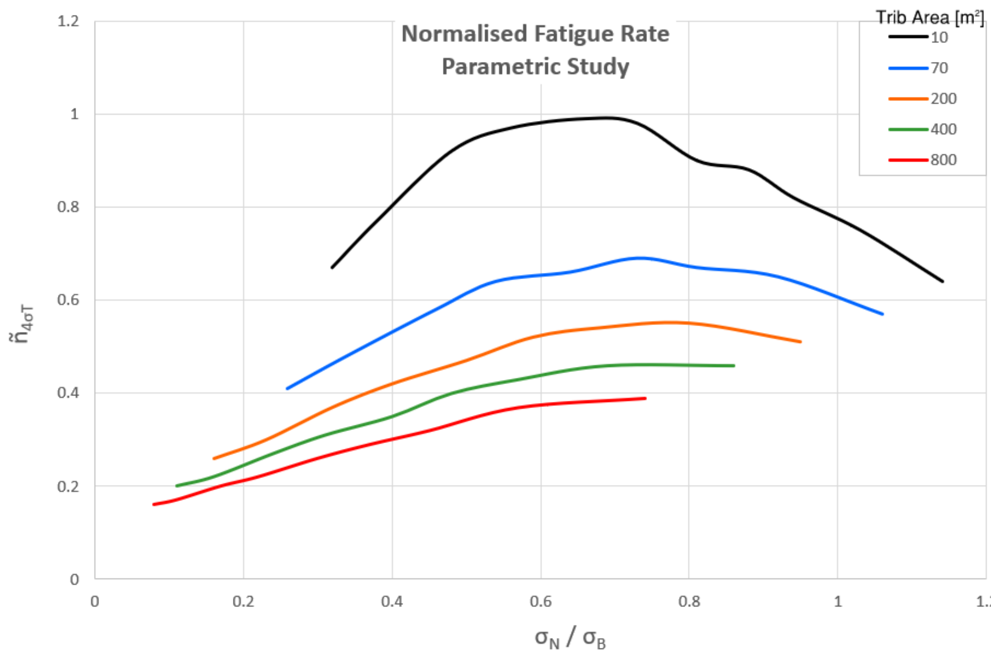


**Figure 2. Normalized Fatigue Rate ( 1% damping)**

The normalized fatigue rate is independent of the mean speed and it is therefore possible to select the relevant $\tilde{n}_{4\sigma T}$ for the structure under consideration, i.e. for a given $\sigma_N$/ $\sigma_B$ and do the summation over the entire wind rose to obtain the cumulative fatigue damage. This methodology, along with additional simplifications on the wind rose, is detailed further in (Wyatt, 2004) and could offer an alternative to the existing codified method, although it would require various curves as shown in Figure 2 and/or a level of rationalization, which is not presented here. Instead, the section below proposes another simpler option adapted to an existing method.

## COMPARISON WITH NARROW-BAND PROCESS (BASIS FOR AS/NZS 1170.2)

The cycles count shown in AS/NZS1170.2 or Eurocode is based on a closed-form distribution of the stress range (Rayleigh distribution), normally applicable to a narrow-band process and with further assumptions on the rms of the stress fluctuation (rms proportional to $\bar{U}^{2.5}$) as in (Holmes, 2012). It is instructive to compare the fatigue damage distribution calculated from the time series and that using the Rayleigh distribution, assuming the same rms $\sigma_T$ in the Rayleigh distribution as for the time series. Figure 3 below provides a comparison of the distribution of damage for two types of structures.

For a very dynamic structure (right), i.e. $\sigma_N$ / $\sigma_B$ > 1.5, the two distributions are shown to match reasonably well. However, for a structure moderately dynamic (left), i.e. $\sigma_N$ / $\sigma_B$ =0.6, the distributions are shown to differ, with that for the closed-form narrowband process over-estimating the cycle counts significantly, as already mentioned by (Holmes, 2012). Therefore, the cumulative counts obtained by summing up $n_{4\sigma T}$ across the stress ranges is significantly higher for the narrow-band process than for the time series.

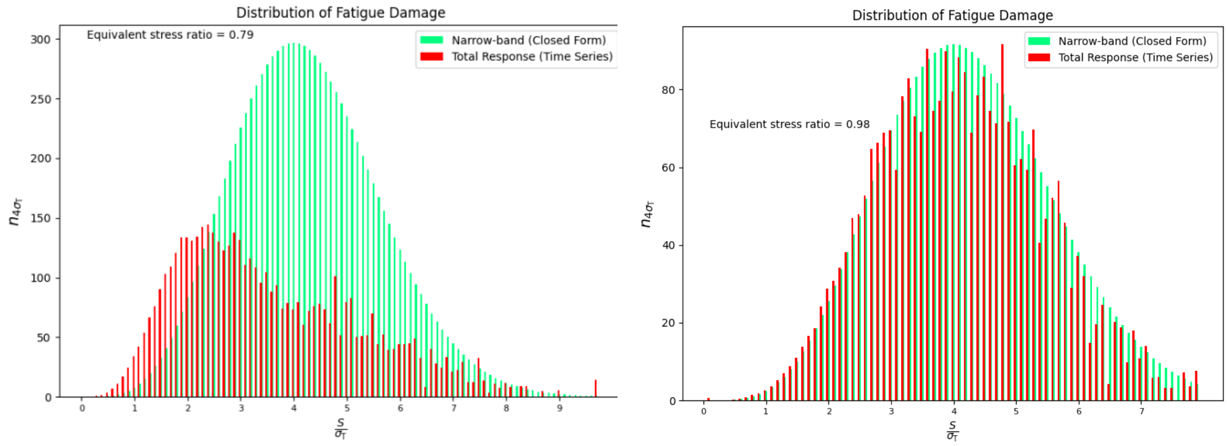


**Figure 3. Comparison of Damage Distribution for Moderately Dynamic (Left) and Very Dynamic Structure (Right)**

Using Equation 2, the difference in cycle counts $n_{4\sigma T}$ highlighted above can be expressed as an equivalent variation in stress resulting in a similar fatigue damage. In the examples shown above, the difference in cycle counts is equivalent to a stress variation of 0.8 for the moderately dynamic structure and close to 1 for the dynamic structure. This stress variation is unsensitive to the mean speeds and is equivalent to shifting the S-N fatigue curve under consideration upwards on the traditional S-N curves plot. The total fatigue damage is therefore less sensitive to the exact cycle count distribution, as long as the design data referred for the fatigue assessment is the stress rather than the cycle counts. In (Holmes et al., 2012) a simple and efficient method is proposed using the cycle counts of AS/NZS 1170.2 and the S-N curves. In addition of its simplicity, its other strength is that the design rule focuses on the stress rather than the cycle counts. Based on the above, it is possible to compensate for the inaccuracy in the damage distribution for moderately or non-dynamic structures.

We tentatively propose conservative reduction factors $R_{Fatigue}$ to the design rule by (Holmes et al., 2012) which may be generalized provided additional checks on sensitivity to turbulence intensity, the bi-slope m exponent of the S-N fatigue curve, and the impact of the assumptions on the narrow-band process parameters. Also note that $R_{Fatigue}$ is shown to gradually reduce from 1 to about 0.6 but were rationalized below, which could also be improved.

$R_{Fatigue}$ * $S_{max}$ < 3.65 * Detail Category for typical S-N curves in the AS Standard.

**Table 1. Reduction Factor for Fatigue**

| $\sigma_N$ / $\sigma_B$ | $R_{Fatigue}$ |
|---|---|
| ≥ 1 | 1 |
| ≤ 0.5 and < 1 | 0.9 |
| < 0.5 | 0.8 |

## References

T.A. Wyatt, Determination of gust action stress cycle counts for fatigue checking of line-like steel structures, *Journal of Wind Engineering and Industrial Aerodynamics*, Volume 92, Issue 5,2004

Holmes J.D., Genner D.,Wind-induced fatigue of steel structures: a simplified design approach to AS 4100. Steel Construction. 2012,45, pp. 2-11. *Journal of the Australian Steel Institute*.

Holmes J.D., Wind-induced Fatigue Cycle Counts – Sensitivity to Wind Climate and Dynamic Response. 7th International Congress of Croatian Society of Mechanics, Zadar, Croatia, 22-25 May 2012.